

Engineering Notes

Transition-Flow-Occurrence Estimation: A New Method

Paul-Dan Silisteanu* and Ruxandra M. Botez†
*École de Technologie Supérieure,
Montréal, Québec H3C 1K3, Canada*

DOI: 10.2514/1.44698

I. Introduction

TRANSITION from a laminar to turbulent regime has been an important topic in aerodynamics since the publication of the pioneering paper of Osborne Reynolds [1] in 1883. A century later we still do not have a complete transition theory; until today the use of empirical correlations or expensive wind-tunnel experiments was mandatory for the practical aerodynamicist.

The classical engineering approach for the transition region modeling numerical aerodynamic calculations is the use of an iterative methodology combining a panel code with a boundary-layer code; for modeling the transition region the boundary-layer code must be coupled with a stability code based on linear stability theory or on empirical correlations; however, this approach could be used only in a limited numbers of flows, as the classical boundary-layer theory is valid only for attached flows [2].

The linear-stability theory can successfully predict the transition onset but offers no information about the transition extent. The main disadvantage of this theory is that it relies on boundary-layer calculations; this makes the methodology unsuitable for being included in a general unstructured computational fluid dynamics (CFD) code [3].

Empirical correlations relating the transition onset with boundary-layer calculations were widely used in industrial calculations: typical examples are the Granville method, the one-step method of Michel, the method of Wazzan, and (probably the most used empirical methodology today in large-scale industrial calculation) the e^N method (on all these methods, see [4]). All the above experimental correlations require accurate boundary-layer calculations, which restrict their use to the range of applicability of the boundary-layer theory [2].

The modern approach is to use a CFD solver for modeling the flow around an aerodynamic configuration. The governing flow equations are the Navier–Stokes equations, which are nonlinear partial differential equations, and we are able to obtain analytical solutions for these equations only for very simple geometries. For arbitrary complex geometries, we rely on numerical solutions of these equations. Unfortunately, with today’s computers, we could not obtain even a numerical solution of these equations for large Reynolds numbers, at least not in industrial applications.

A direct Navier–Stokes simulation of an entire airplane at a practical Reynolds number is impossible in the actual stage of

computer development. A simplification of the problem can be obtained by filtering the governing flow equations; the obtained mathematical model still retains the main flow characteristics. The Navier–Stokes equations can be filtered spatially (large-eddy simulations) or temporally [Reynolds-averaged Navier–Stokes (RANS)]; the first technique is capable of retaining more from the flow physics but is still in its infancy as an industrially accepted methodology. The RANS equations are the workhorse of today’s aerodynamic engineer; they can correctly predict only the flow turbulent regions. If the flow contains laminar regions, RANS will overpredict the airplane skin-friction and drag coefficients. In cases when the precise prediction of the drag force is required, one cannot rely entirely on RANS equations.

Recently, there was an attempt to circumvent the problem of using empirical correlations in a general CFD code by using two transport equations in addition to a turbulence model [5]. The first equation models an intermittence function used to trigger the transition, and the second uses the momentum-thickness Reynolds-number Re_θ parameter used by most empirical correlations.

In this paper we propose a general methodology for detecting the transition onset and extent from the temporal variation of the skin-friction coefficient. The present methodology is validated with experimental data for two-dimensional subsonic configurations. To test the robustness of the proposed method we use the Ansys Fluent 6.3 flow solver. By comparison of the drag obtained with a fully turbulent simulation on the entire domain using RANS simulation with the drag obtained with the present methodology vs the experimental data, we observe a better drag prediction for the proposed methodology. The new methodology can also be extended in a straightforward manner to three-dimensional configurations.

II. Numerical Setup

In the present paper we propose an iterative methodology for taking into account the transition effects in a general-purpose CFD solver. To be self-contained the methodology will use only data directly available from a numerical simulation of this type. No boundary-layer parameters or empirical correlations are used in the present method.

The first step of the method is used for determining the transition onset and the transition length on an airfoil; in a second step we split the computational mesh in three regions: a laminar, transition, and turbulent region. A schematic view of this procedure is presented in Fig. 1.

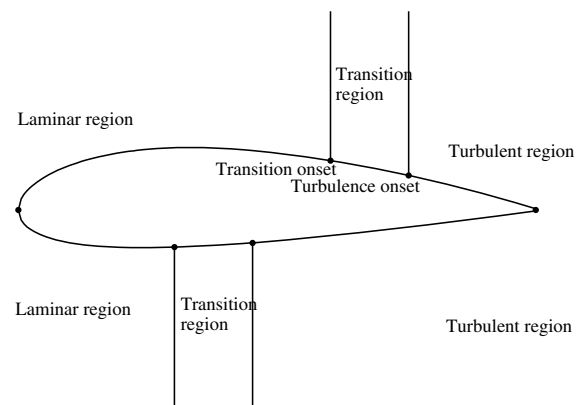


Fig. 1 Flow regions around an airfoil.

Received 1 April 2009; revision received 15 December 2009; accepted for publication 21 December 2009. Copyright © 2010 by Ruxandra Mihaela Botez. Published by the American Institute of Aeronautics and Astronautics, Inc., with permission. Copies of this paper may be made for personal or internal use, on condition that the copier pay the \$10.00 per-copy fee to the Copyright Clearance Center, Inc., 222 Rosewood Drive, Danvers, MA 01923; include the code 0021-8669/10 and \$10.00 in correspondence with the CCC.

*PhD Student, Laboratory of Research in Active Controls, Avionics, and AeroServoElasticity LARCASE, 1100 Notre-Dame West St. Member AIAA.

†Professor, Laboratory of Research in Active Controls, Avionics, and AeroServoElasticity LARCASE, 1100 Notre-Dame West St. Member AIAA.

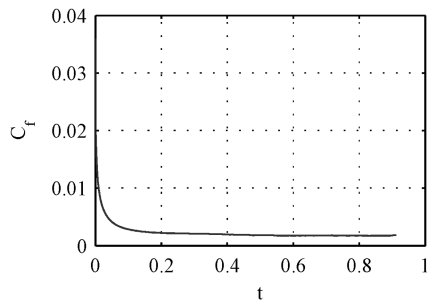
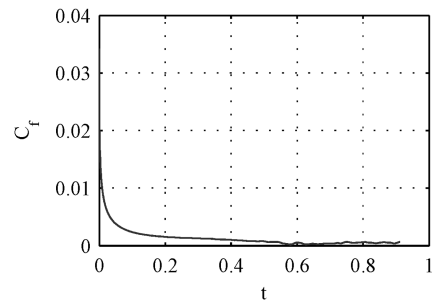
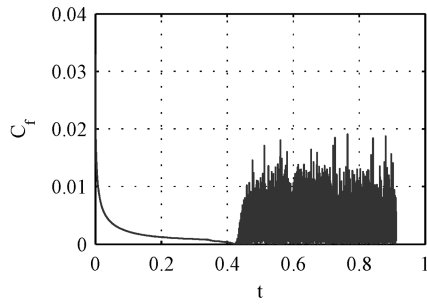
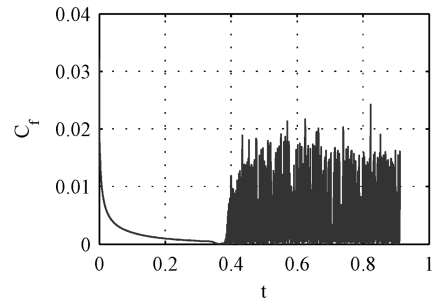
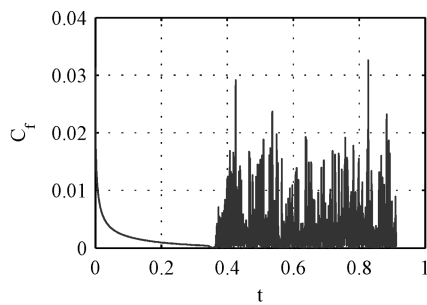
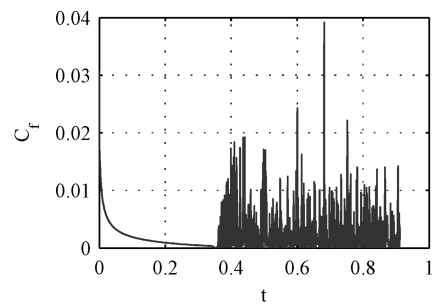
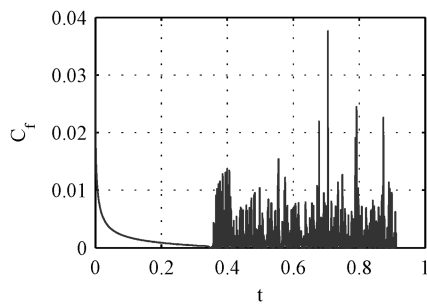
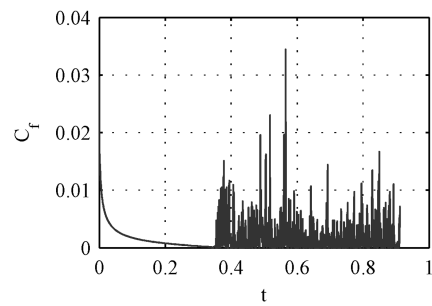
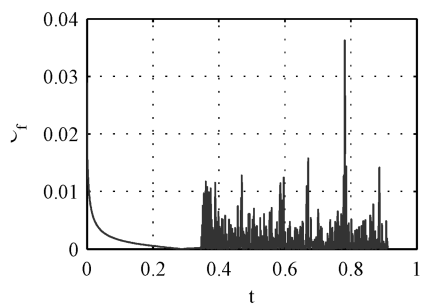
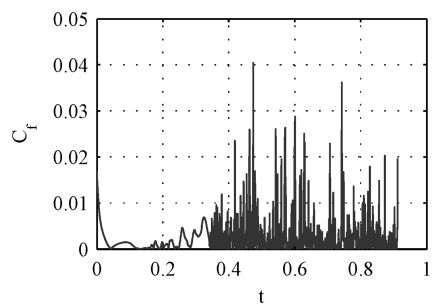
a) 10% of x/c b) 20% of x/c c) 30% of x/c d) 40% of x/c e) 50% of x/c f) 60% of x/c g) 70% of x/c h) 80% of x/c i) 90% of x/c j) 100% of x/c

Fig. 2 Time history of the skin-friction coefficient at different locations on the airfoil upper side.

For the first step of the method we simulate the unsteady flow around an airfoil without the use of a turbulence model. We must note that this is not an accurate direct Navier–Stokes simulation; this step of the method is only used for determining the transition and turbulence onset using a general-purpose CFD solver.

The transition-onset location can also be obtained by using the linear theory of hydrodynamic stability [3], but this theory does not offer any information about the transition length and the turbulence onset. Also, we cannot include in a straightforward manner a stability code in a general CFD code; for solving the linear stability equation we need boundary-layer parameters that cannot be directly extracted from a CFD solution.

The second step of the method consists in an unsteady RANS simulation on the three regions of the flow: in the laminar region, the dynamic-viscosity μ_T quantity is set to zero; in the turbulent region, μ_T is calculated from the Spalart–Almaras turbulence model [6]. The coupling between the laminar and turbulent region is done by the use of a linear intermittence function Γ , which is zero at the transition onset and one at the turbulence onset; this function multiplies the dynamic viscosity.

The present method uses the temporal variation of the skin-friction coefficient for the transition-onset prediction. In the laminar region of the flow the temporal variation is smooth; on the other hand, in the turbulent region this variation is highly irregular.

A typical example of the C_f variation on the upper surface of the NACA 2415 airfoil is presented in Fig. 2. These data are obtained for a Reynolds number of 3×10^6 , a Mach number of 0.2, and an incidence of 4° .

It could be observed that the time histories of the skin-friction coefficient became irregular at approximately 30% from the chord on the upper side of the airfoil. A similar situation is present for the skin friction on the lower side of the airfoil: the flow is smooth up to 80% of chord.

To estimate the length of the transition region and the turbulence onset we can use the root mean square (RMS) of the skin-friction coefficient on the airfoil:

$$C_{f_{RMS}} = \sqrt{\frac{1}{N} \sum_{i=1}^N (C_{f_i} - \bar{C}_f)^2} \quad (1)$$

We suppose the turbulence onset is located at the maximum RMS: Fig. 3 for the upper side of the airfoil and Fig. 4 for the lower side of the airfoil.

This step of the proposed method is implemented in the Ansys Fluent 6.3 flow solver with the aids of a user-defined function (UDF). Using the UDF mechanism [7] we could interact with the solver and save the values of C_f and ω at each time step.

To facilitate the meshing of the geometry of interest we have developed a FORTRAN program that uses the Gambit mesh generator of Fluent in an iterative automated manner. This program allows the user to generate an algebraic structured mesh around an airfoil by varying a few parameters such as the length of the domain, the number of points on each side of the domain, and the grid space on the airfoil. The computer program could be used for splitting the grid in three or more (for a multi-element airfoil) regions using as inputs the coordinates of the transition and turbulence onsets (see Fig. 1) obtained in the first stage of the method.

As a rule of thumb we use a domain of 20 chord lengths for the segments AB, OC, and ED and twelve chords for the segments CB, CD, OE, and OA; the details of the grid discretization are problem-dependent. For obtaining an accurate solution in the turbulent region we impose $y^+ = 1$, from which we estimate the distance between the first point in the mesh in the normal direction on the airfoil and the airfoil surface.

The computational mesh has 324,200 cells and 325,771 nodes, with 563 points on the upper side and 558 points on the lower side of the airfoil. Referring to Fig. 5 we have 250 nodes on the AB, OC, and ED; 200 nodes on the OA, CB, CD, and OE; 563 nodes on the FA; and 558 nodes on the FE.

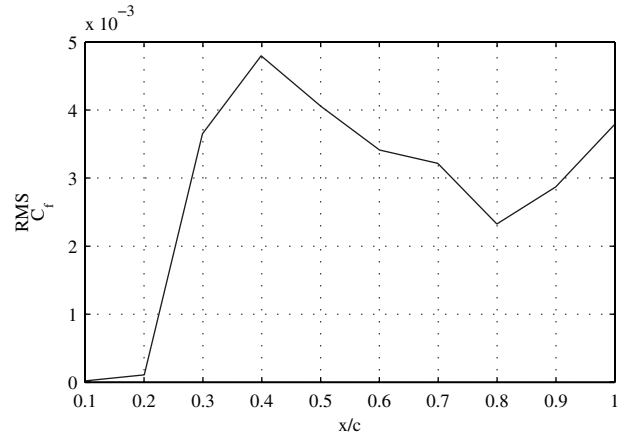


Fig. 3 RMS of the skin-friction coefficient on the airfoil upper side.

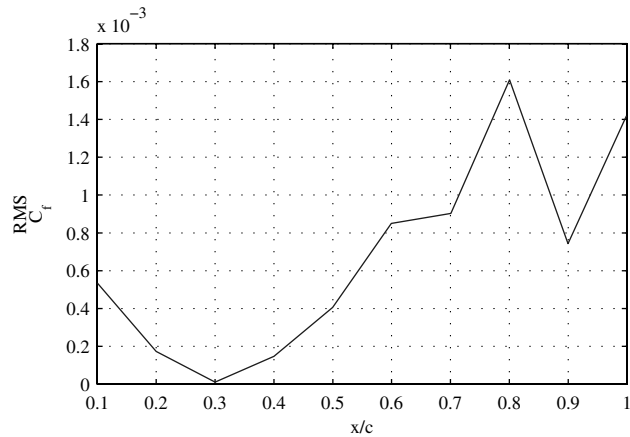


Fig. 4 RMS of the skin-friction coefficient on the airfoil lower side.

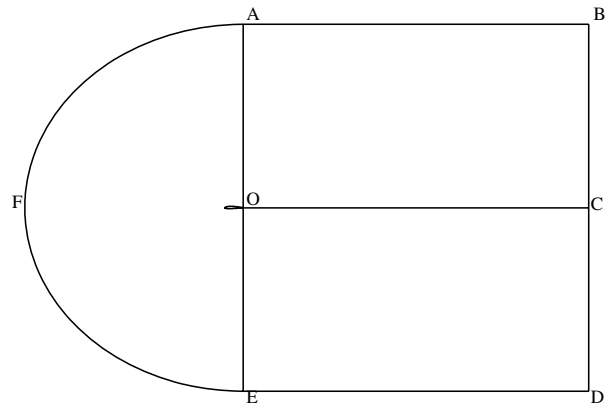


Fig. 5 A generic computational domain.

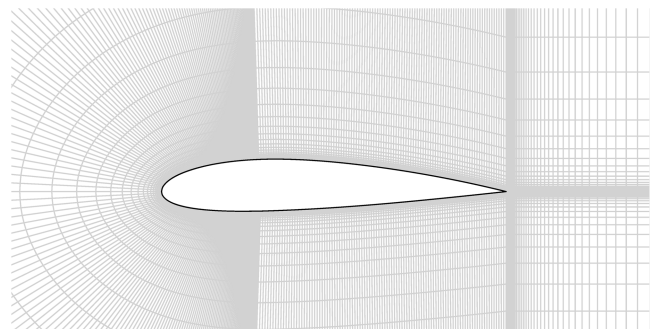


Fig. 6 Closed view of the airfoil mesh (each second line of the original mesh was removed).

The grid spacing in the normal direction from the airfoil is $\Delta y = 0.00005$ in order to satisfy the $y^+ = 1$ condition, and is $\Delta x = 0.002$ in the chordwise x direction; the chord dimension is one (see Fig. 6).

The solver used for this validation is the pressure-based solver of Fluent 6.3. The time discretization of the flow equations is done with a second-order implicit algorithm and a time step of $\Delta t = 0.0001$ s.

For the spatial discretization we have used the scheme of pressure implicit with splitting of operators (PISO) [7], with second order for the pressure and third order for the other quantities. The PISO scheme is a pressure-velocity calculation procedure especially adequate for unsteady flows.

The boundary conditions used are velocity inlet for the BAFED frontier (see Fig. 5), pressure outlet for BCD, and on the airfoil the wall condition.

III. Experimental Validation and Generalization of the Present Methodology on Various Cases

To validate the present methodology two airfoils are used as test cases: a classical NACA 2415 airfoil, for which there are in literature experimental data [8], and a laminar airfoil NLF(1)-0416 [9].

The first test case uses a NACA 2415 airfoil presented in the classical compilation of experimental test cases of Abbott and

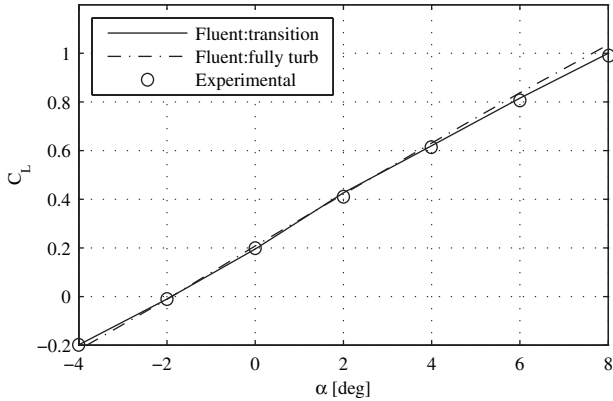


Fig. 7 Lift coefficient vs angle of attack for NACA 2415 at $Re = 3 \times 10^6$ and $M = 0.2$.

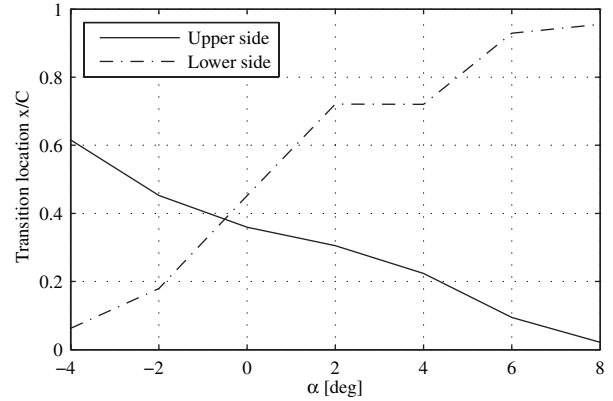


Fig. 10 Transition position vs incidence for NACA 2415 at $Re = 3 \times 10^6$ and $M = 0.2$.

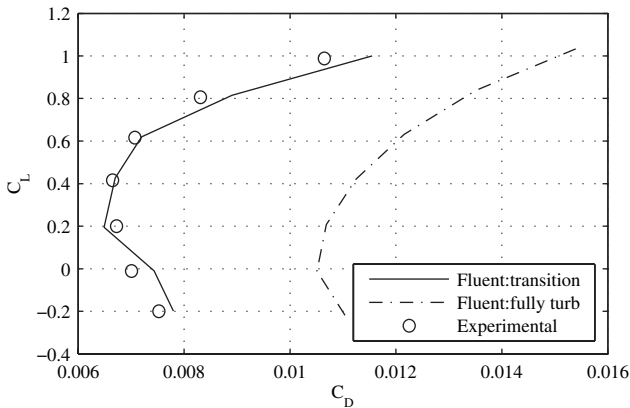


Fig. 8 Lift coefficient vs drag coefficient for NACA 2415 at $Re = 3 \times 10^6$ and $M = 0.2$.

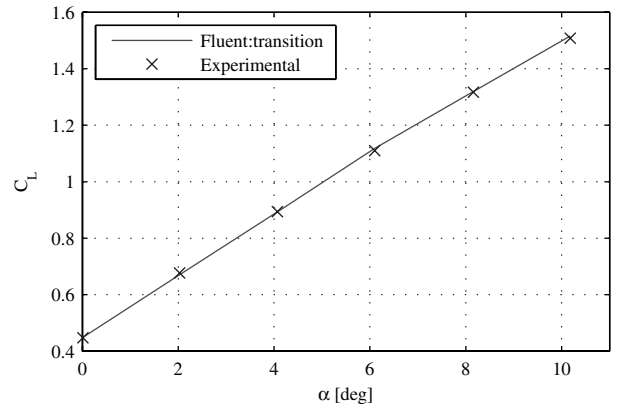


Fig. 11 Lift coefficient for NLF(1)-0416 airfoil at $Re = 4 \times 10^6$ and $M = 0.1$.

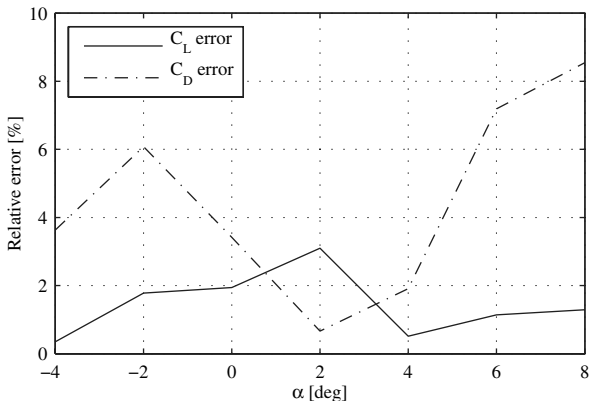


Fig. 9 Relative error for the lift and drag coefficients for NACA 2415 at $Re = 3 \times 10^6$ and $M = 0.2$.

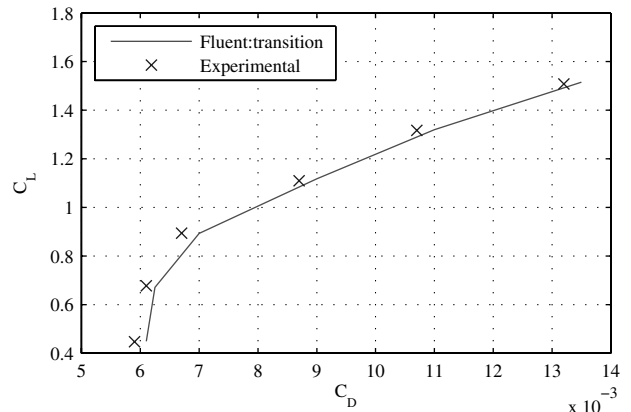


Fig. 12 Lift coefficient vs drag coefficient for NLF(1)-0416 airfoil at $Re = 4 \times 10^6$ and $M = 0.1$.

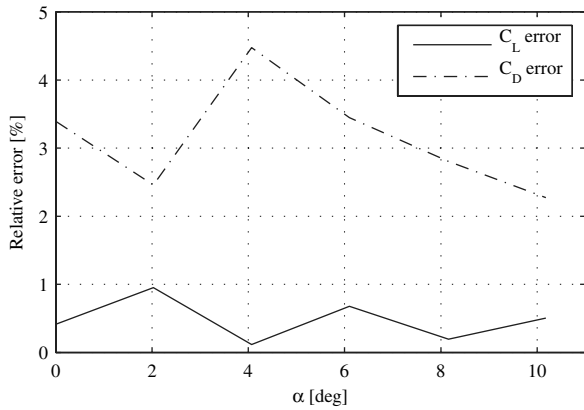


Fig. 13 Relative error for the lift and drag coefficients for NLF(1)-0416 airfoil at $Re = 4 \times 10^6$ and $M = 0.1$.

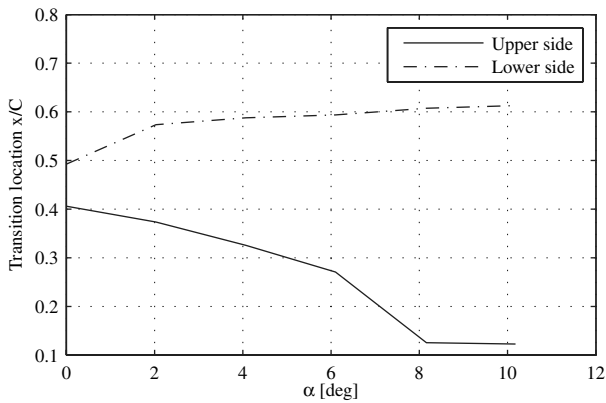


Fig. 14 Transition position vs incidence for NLF(1)-0416 airfoil at $Re = 4 \times 10^6$ and $M = 0.1$.

Doenhof [8]. The given experimental conditions are the Reynolds number 3×10^6 and the incidence of the airfoil between -4° and 8° ; the Mach number used in the simulation was 0.2.

In Fig. 7 we compare the results obtained with the present method with experimental data. We can note that the effect of the transition is not very important for C_L ; the results obtained for a fully turbulent simulation are almost identical to the results obtained in the presence of transition.

For the case of the drag coefficient (see Fig. 8) the results obtained from a fully turbulent simulation are 50% overestimated. This large error can be explained by the fact that at this flow condition the laminar part of the flow is very large: around 80% of the lower side of the airfoil at an incidence of 4° for example.

The lift and drag coefficients relative errors calculated with the new method vs experimental data are presented in Fig. 9. The lift coefficient relative error is under 4%, and the drag coefficient relative error is lower than 8%.

The transition-onset position on the NACA 2415 airfoil vs the angle of attack (Fig. 10) shows a smoother evolution for the upper side of the airfoil than for the lower side.

For the second test case we have used a laminar airfoil NLF(1)-0416 designed for maintaining the laminar region of the flow over

30% from chord. The experimental conditions were: a Mach number of 0.1, a Reynolds number of 4×10^6 , and incidence angles from 0 to 10° .

The results obtained for the lift and drag coefficients vs the experimental data are presented in the next two figures (Figs. 11 and 12).

Relative errors obtained for the lift and drag coefficients variations with angles of attack for the NLF(1)-0416 airfoil (Fig. 13) are smaller than the errors obtained for the NACA 2415 airfoil, due probably to the fact that experimental testing for the NLF(1)-0416 airfoil took place more recently than the experimental tests on the NACA 2415 airfoil.

From Fig. 14 we can observe that the laminar part of the flow is larger than 30% for angles smaller than 4° for the upper side of the airfoil, and larger than 50% for the airfoil lower side on the entire range of angles of attack of 0 to 10° .

IV. Conclusions

A new method for transition estimation has been presented. The new method can successfully predict the drag coefficient of an airfoil configuration in the frame of a general CFD code. Comparing the results obtained with the present method with the classical approach of using only RANS calculation in the entire flow domain (Fig. 5), the present method predicts the parameter of interest for the aerodynamicist with good accuracy.

A plus of the present methodology is that it does not use empirical correlations for detecting the transition.

The method can be extended to three-dimensional configurations in a straightforward way.

A future extension of the method will be to compressible flows and especially to transonic-aerodynamics calculations. In a preliminary set of tests the authors have obtained good results using the RMS of the skin friction for a transonic two-dimensional airfoil.

References

- [1] Reynolds, O., "An Experimental Investigation of the Circumstances Which Determine Whether the Motion of Water Shall Be Direct or Sinuous, and of the Law of Resistance in Parallel Channels," *Philosophical Transactions of the Royal Society of London*, Vol. 174, 1883, pp. 935–982. doi:10.1098/rstl.1883.0029
- [2] Schlichting, H., and Gersten, K., *Boundary-Layer Theory*, Springer-Verlag, New York, 2001.
- [3] Cebeci, T., Shao, J. P., Kafyeke, F., and Laurendeau, E., *Computational Fluid Dynamics for Engineers*, Springer-Verlag, New York, 2005, Chaps. 8, 11.
- [4] White, F., *Viscous Fluid Flow*, McGraw-Hill, New York, 2005.
- [5] Menter, F. R., Langtry, R. B., Likki, S. R., Suzen, Y. B., Huang, P. G., and Volker, S., "A Correlation-Based Transition Model Using Local Variables. Part 1: Model Formulation," *Journal of Turbomachinery*, Vol. 128, No. 3, 2006, pp. 413–422. doi:10.1115/1.2184352
- [6] Spalart, P. R., and Allmaras, S. R., "A One-Equation Turbulence Model for Aerodynamic Flows," AIAA Paper 92-0439, 1992.
- [7] <http://www.fluentusers.com>.
- [8] Abbott, I., and Doenhof, A., *Theory of Wing Sections, Including a Summary of Airfoil Data*, Dover, New York, 1959.
- [9] Somers, D. M., "Design and Experimental Results for a Natural-Laminar-Flow Airfoil for General Aviation Applications," NASA TP 1861, 1981.